Journal of Hazardous Materials 499 (2025) 140176

Contents lists available at ScienceDirect

Journal of Hazardous Materials

journal homepage: www.elsevier.com/locate/jhazmat

Synergistic mineralization of the UV filter benzophenone-3 by a cross-feeding consortium from wastewater treatment plants: Insights into novel pathway and bioremediation strategy

Ao Zhang, Piaopiao Pan, Ning-Yi Zhou, Tao Li *

State Key Laboratory of Microbial Metabolism, Joint International Research Laboratory of Metabolic and Developmental Sciences, and School of Life Sciences and Biotechnology, Shanghai Jiao Tong University, Shanghai 200240, China

HIGHLIGHTS

- Bacteria degrade UV filter benzophenone-3 (BP-3) through a C-C bond cleavage pathway.
- A consortium consisting of *Pigmentiphaga* and *Brucella* synergistically degrades BP-3.
- Two BP-3 catabolic intermediates 3-methoxyphenol and benzoate are identified.
- Integration of metagenome and consortia reconstruction reveals metabolic interaction.

GRAPHICAL ABSTRACT

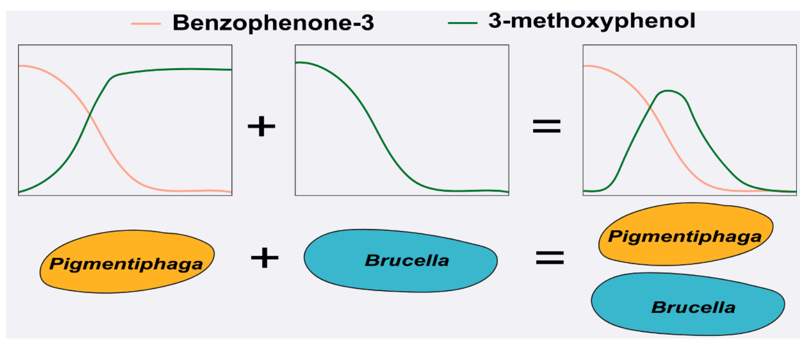

ARTICLE INFO

Keywords:
Benzophenone-3
Biodegradation
Microbial consortia
Organic UV filters
Wastewater treatment

ABSTRACT

Benzophenone-3 (BP-3), used as an organic UV filter in diverse consumer products including cosmetics, has been frequently detected in wastewater treatment plants (WWTPs) and aquatic environments. BP-3 and its transformation products are regarded as emerging micropollutants due to their low biodegradability. Here, we investigate the synergistic degradation of BP-3 by a bacterial consortium seeded from aerobic sludge WWTPs. BP-3 is found to be initially degraded through a novel pathway involving a C-C bond cleavage step, producing intermediates 3-methoxyphenol (3MOP) and benzoate, two naturally occurring compounds which can be readily degraded in the environment. Metagenome-guided pure culture isolation and pathway analysis reveal that bacterial strains from genera *Pigmentiphaga* and *Brucella* synergistically contribute to the BP-3 mineralization. Specifically, the *Pigmentiphaga* strain degrades BP-3 into benzoate and 3MOP, with the former being utilized by itself and the latter utilized by the *Brucella* strain. A reconstructed consortium, consisting of two isolated strains from *Pigmentiphaga* and *Brucella*, exhibits similar degradation performance to that of the natural consortium, indicating their crucial roles in environmental BP-3 degradation. These findings provide new insights into BP-3 biodegradation at the microbial community level, offering potential strategies for wastewater treatment applications by manipulating synthetic microbial consortia.

* Correspondence to: Life Science Building, Shanghai Jiao Tong University Nr 800, Dongchuan Rd, Shanghai 200240, PR China.
E-mail address: lisuitao@sjtu.edu.cn (T. Li).

https://doi.org/10.1016/j.jhazmat.2025.140176
Received 4 August 2025; Received in revised form 25 September 2025; Accepted 16 October 2025
Available online 17 October 2025
0304-3894/

1. Introduction

Organic micropollutants, including personal care products, pharmaceuticals and pesticides, are continuously discharged into municipal wastewater treatment plants (WWTPs) through anthropogenic activities. However, a large portion of micropollutants cannot be removed by the current WWTPs treatment processes, resulting in their frequent detection in effluents and subsequent dispersion into various aquatic environments. Bacteria can evolve specific mechanisms to tackle micropollutants, and show a potential for wastewater treatment [1]. But the evolution of a complete catabolic pathway toward a new micropollutant is rather challenging for bacteria within a relatively short timeframe. As a result, bacteria can frequently adopt a synergistic way to utilize micropollutants within a consortium, thus removing them from the environment [2]. Nonetheless, the metabolic interactions among the strains within bacterial consortia during micropollutants degradation process are far from being understood.

Oxybenzone (2-hydroxy-4-methoxybenzophenone, benzophenone-3, or BP-3), belonging to the class of aromatic ketones, is an excellent ultraviolet filter (UVF) compound firstly synthesized in 1906 [3]. It has been widely used in sunscreen formulations to avoid skin damage, or in plastics and other consumer products to prevent photodegradation. BP-3 is one of the most commonly used UVFs and has been listed as a "high-production-volume chemical" [4]. The photochemically stable and lipophilic properties of BP-3 lead to its accumulation in the environment such as sediments, seawater, tap water, rivers, sewage sludges, and soils [5–8]. Ultimately, they could be accumulated in plants, and then to animals and humans through food chain [9–12]. BP-3 is one of the most frequently detected UVFs in the environment around the world, with concentrations ranging from ng/L to mg/L. The widespread occurrence of BP-3 in the environment raises our concerns about its potential risks for the following reasons: i) BP-3 has been reported to be an endocrine disruptor that potentially leads to fertility defects [13], cancerous tumors, and development disorders to humans [10,14]; ii) BP-3 has been shown to exert adverse effects including neurotoxicity, genotoxicity, and cytotoxicity on wildlife [9,15]; iii) BP-3 also possibly plays a role on causing coral bleaching [16,17].

In light of the environmental threats posed by BP-3, significant attention over the past decade has been directed toward investigating its physiochemical and biological transformation processes of BP-3 (Fig. 1) [18]. Evidence indicates that BP-3 undergoes transformation into brominated disinfection byproducts in seawater swimming pools following chlorination disinfection treatments [19,20]. Additionally, the photo-transformation of BP-3 yields numerous transformation products, many of which exhibit markedly higher toxicity than their parent compound BP-3 [21]. In aquatic organisms, one of the main BP-3 metabolites, i.e., benzophenone-8, is shown to be likely more toxic than BP-3 [22]. Microbial degradation has emerged as a notable approach contributing to BP-3 transformation in complex environments, such as during soil aquifer treatment [23] or within domestic wastewater treatment plants (WWTPs) [5,24]. Different bacterial consortia or strains, including *Sphingomonas wittichii* strain BP14P [25], *Rhodococcus* sp. S2–17 [26], and *Methylophilus* sp. strain FP-6 [27], have been reported for their capacity to degrade BP-3. Diverse biodegradation pathways are proposed and most of them are featured with the formation of either demethylated intermediate benzophenone-1 (BP-1) or various ring-hydroxylating products from BP-3. For example, *Rhodococcus* sp. S2–17 contains a cytochrome P450 enzyme to initiate the demethylation of BP-3 into BP-1. However, microbes responsible for the direct cleavage of BP-3 had not been characterized before this study (Fig. 1). Biodegradation of BP-3 is one of the main pathways for its transformation in the environment, the degradation of BP-3 and its derivatives by environmental microbial community holds significant potential for the bioremediation of BP-3 polluted environments [28]. However, critical knowledge gaps remain in how complex environmental microbial community cooperate to remove this difficult-to-biodegrade compound.

As part of our systematical assessment project related to the degradation capability and mechanism of microbes from WWTPs toward pharmaceuticals and personal care products (PPCPs) [29,30], we here investigated the biodegradation process of BP-3 by enriching a BP-3-degrading consortium seeded from the wastewater of a WWTP in Shanghai (China). An efficient BP-3-degrading consortium was enriched and characterized by metagenomic sequencing. Moreover, the keystone strains of this consortium were isolated and identified to be the ones belonging to *Pigmentiphaga* and *Brucella*. Based on the results from catabolic intermediates using the ultrahigh resolution mass spectrometer, metagenomic assembly, and reconstruction of the BP-3-degrading consortium, we revealed a novel BP-3 breakdown manner initialized by a direct C-C bond cleavage step which has not been previously found

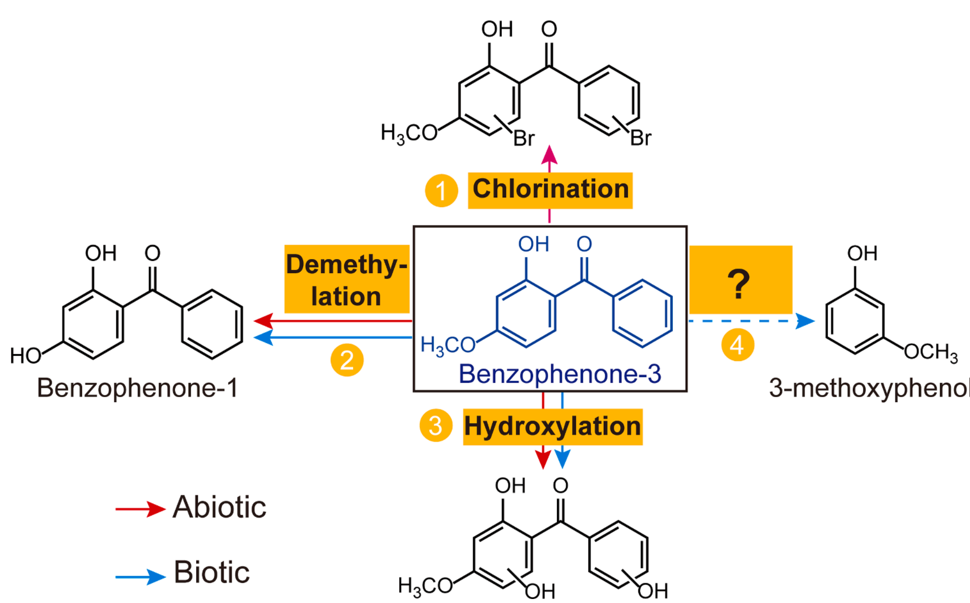

Fig. 1. The proposed abiotic and biotic transformation processes of benzophenone-3 (BP-3) in the environment. (1) Transformation of BP-3 into toxic brominated byproducts during chlorination disinfection treatments; (2) Abiotic and biotic demethylation of BP-3; (3) Abiotic and biotic hydroxylation of BP-3; (4) A novel BP-3 biodegradation process proposed in this study.

in environmental microbes. Eventually, the degradation kinetics, and performance in real wastewater with the single strains and synthetic consortium were further estimated.

2. Materials and methods

2.1. Reagents and media

Benzophenone-3 with a purity of >98 % was purchased from Sigma-Aldrich (St. Louis, USA), benzoic acid and 3-methoxyphenol (97 % purity) was obtained from BiDe Pharmaceutical Technology Co., Ltd (Shanghai, China). All HPLC-grade solvents were obtained from Inno-Chem (Beijing, China). Nitrogen-free minimal salts medium (MSM) consisted of (per liter) 14.3 g $Na_2HPO_4{\cdot}12H_2O$, 3 g KH_2PO_4, 0.3 mg $FeSO_4{\cdot}7H_2O$, 0.06 mg $MgSO_4{\cdot}7H_2O$, 0.28 mg $MnSO_4{\cdot}H_2O$, 1 mg $CaCl_2$, 0.05 mg $ZnSO_4$, 0.05 mg $CuSO_4$ and 0.05 mg H_3BO_3, at pH 7.0. MSM was supplemented with 0.2 % (w/v) ammonium sulfate as a nitrogen source when necessary. The 1/5 strength tryptic soy broth (TSB) was used as rich medium to culture bacterial isolates in this study. Solid plates were prepared by adding 1.5 % agar.

2.2. Aerobic enrichment culture

Aerobic liquid microcosms were established in 250 mL Erlenmeyer flasks, each containing 150 mL of nitrogen-containing MSM, 1.5 g of activated sludge from the aeration tank of a domestic WWTP, and 200 μM BP-3 as the sole carbon source. Control experiments were prepared with autoclaved activated sludge under same conditions. The microcosms were incubated at 30 °C in a shaking incubator at 180 rpm and the enrichment culture was transferred monthly to 150 mL fresh nitrogen-containing MSM with 200 μM BP-3. BP-3 was regularly refed at 10 and 20 days for each transfer. After four-month enrichment, the enriched culture was continuously passaged by weekly inoculating (1 %, v/v) to 150 mL fresh nitrogen-containing MSM with 200 μM BP-3. Metagenome sequencing and BP-3 degradation assays of two consecutively transferred enrichment cultures (T1 and T2) were conducted as described below.

2.3. Metagenome analysis

During the enrichment assays, 50 mL of enrichment cultures from two transfers were sampled once BP-3 was completely degraded. The bacterial cells were collected by centrifugation at 13, 000 g for 10 min at 4 ℃. DNA extraction from the collected bacterial pellet was performed using FastDNA SPIN kit (Q-Biogene, CA, USA) according to the manufacturer's instructions. The extracted DNA was fragmented into ~350 bp lengths, and fragment DNA libraries were constructed for metagenomic sequencing using the Illumina HiSeq platform (Illumina, CA, USA). The base-calling pipeline was used to process the raw fluorescence images and call sequences. The raw read length was trimmed to 150 bp and low-quality nucleotides (quality value < 20) were discarded. The trimmed paired-end reads from the two transfers were assembled individually by CLCbio de novo assembly algorithm, with a k-mer size of 63 and a minimum contig length of 1 kbp. A binning process was applied to recover the genomes of dominant species from the metagenomes. CheckM (version 1.0.11) was used to evaluate the genome completeness using marker genes. The assembled scaffolds were submitted to Meta-Prodigal (version 2.6.3) for open reading frame (ORF) prediction. ORFs were further subjected to BLASTx against the NCBI-nr database with an e-value of $1e^{-5}$ for functional annotation and taxonomic annotation.

2.4. Isolation and characterization of pure strains from the enrichment culture

The aforementioned BP-3-degrading enrichment culture was serially diluted and spread on TSB agar plates, then incubated at 20 ℃ for three days. The colonies on the plates displayed two distinct morphologies, and three colonies for each type were inoculated into TSB liquid media for growth, and stock cultures were stored in 50 % glycerol at -80 ℃ for future use. Species identification was performed for all pure isolates by amplifying and sequencing the 16S rRNA gene sequences using primers 27 F (5′-AGAGTTTGATCCTGGCTCAG-3′) and 1492 R (5′-TACGACTTAACCCCAATCGC-3′). A phylogenetic tree based on the 16S rRNA gene sequences was constructed by the MEGA11 (v11.0.13) using the maximum likelihood method [31]. To validate their growth capacities on BP-3 or 3MOP, the isolates were individually spiked into nitrogen-containing MSM, supplemented with 0.1 mM BP-3 or 3MOP as the sole carbon source, and incubated at 30 ℃ in a shaking incubator at 180 rpm.

Scanning electron microscopy (SEM) was used to observe the cell morphology of the bacterial isolates. Specifically, fresh colonies on TSB plates were inoculated and cultivated overnight in TSB liquid medium at 30 ℃, 180 rpm. Cells were collected by centrifugation (5000 g, 5 min), and washed with MSM three times. The bacterial cells were fixed with formaldehyde and sequentially treated with 30 %, 50 %, 70 %, and finally 90 % of ethanol for dehydration. The dehydrated cells were lyophilized to form bacterial powder and coated with a thin layer of gold on the surface before SEM inspection. All samples were imaged using a Rise Magna Scanning Electron Microscope (Tescan, Czech Republic) under high vacuum at 5 keV.

2.5. Growth and degradation experiments

For liquid culture, BP-3 in ethyl acetate was added to a sterile glass tube, and the solvent was completely evaporated before adding sterile MSM. 3MOP was added to the MSM to achieve the desired concentration using a 5 mM aquatic stock solution. A 1 % inoculum was used to prepare fresh culture in MSM supplemented with 100 μM BP-3. Bacterial growth on BP-3 or 3MOP was indicated by the optical density at 600 nm ($OD_{600\ nm}$) and counting colony-forming units (CFUs). $OD_{600\ nm}$ was measured using a spark multimode microplate reader. CFUs were counted at appropriate time points by spreading the serially diluted cultures on TSB plates and incubating for 36 h.

In order to identify the intermediates derived from the biodegradation of BP-3, whole-cell biotransformation and crude cell extract reactions were performed. For whole-cell biotransformation, strain NyZ216 was grown in TSB medium overnight on a rotary shaker and harvested by centrifugation (6000 g, 20 min). After being washed three times with MSM, bacterial cells were resuspended to an $OD_{600\ nm}$ of 1.0 and added with 200 μM BP-3. At appropriate intervals, 1 mL samples were collected and an equal volume of acetonitrile was added to stop the reaction.

To prepare crude extracts, strain NyZ216 were cultivated in nitrogen-containing MSM supplemented with 200 μM BP-3. The cells were collected by centrifuging at 6000 g for 20 min, suspended with 50 mM Tris-HCl buffer (pH 8.0), and disrupted by sonication. The debris was then removed by centrifugation at 17, 000 g for 45 min, and the supernatants were used as crude enzymes (CE). The crude enzyme assay was performed in 5 mL reaction mixture containing 100 mg crude enzymes and 0.1–1 mM BP-3 at 30 ℃, then stopped by adding equal volume of acetonitrile. The supernatants of the reaction mixtures were collected by centrifuging at 17, 000 g for 10 min and subjected to further analysis after filtering through a 0.22-μm filter membrane.

2.6. BP-3 degradation capacities of indigenous microorganisms from different WWTPs

Wastewater samples were collected from 14 municipal WWTPs across China (Table S1). For each wastewater sample, a microcosm was prepared with 5 mL of wastewater and spiked with 1 mM BP-3 as the target pollutant for subsequent experiments. All microcosms were incubated at 30 °C in a shaking incubator at 180 rpm. BP-3 removal rates over the 10-day incubation period were determined by quantifying its concentration in the system. Three parallel experiments were conducted for each sample, with control experiments using the corresponding sterilized wastewater. To monitor BP-3 metabolite formation, 5 mL microcosms of each wastewater sample were incubated under the same conditions. At designated time points (1, 2, 5, 7, and 10 days), 200 μL of liquid was collected and immediately mixed with an equal volume of acetonitrile to quench metabolic activity.

2.7. Performance of reconstructed consortium in real wastewater

Strains NyZ216 and NyZ218 were precultured overnight in TSB under optimal growth conditions. Bacterial cells were harvested by centrifugation, washed with MSM, and resuspended in sterile deionized water to an $OD_{600\ nm}$ of 1.0. A 0.5 % (v/v) inoculum of each bacterial suspension was added to wastewater from municipal WWTP of Lanzhou (China), which is incapable of degrading BP-3. The cultures were supplemented with 0.8 mM BP-3 and incubated at 30 °C with shaking at 180 rpm. Control treatments included natural and sterilized wastewater without bacterial inoculation. Samples were collected every 24 h, and microbial activity was halted by adding an equal volume of acetonitrile. BP-3 concentration was quantified using High Performance Liquid Chromatography (HPLC).

2.8. Analytical methods

BP-3 and 3MOP were quantified by HPLC with an Agilent 1260 Infinity II LC system coupled with a DAD detector. A C_{18} reversed-phase column (4.6 × 250 mm, 5 μm; Agilent technologies., CA, USA) was used and maintained the column temperature at 25 ± 2 °C. The detection wavelengths for BP-3 and 3MOP were 287 nm and 275 nm, respectively. A series of concentrations ranging from 5 to 100 μM of substrates in acetonitrile were used to prepare the standard calibration curves. The mobile phase consisted of water containing 0.1 % (v/v) formic acid (A) and acetonitrile (B). The HPLC method began with 10 % solvent B, followed by a linear gradient increase to 90 % B over 15 min, held for 5 min, then returned to the initial conditions for an additional 5 min to equilibrate the column. Flow rate was set at 0.8 mL/min, and injection volume was 10 μL. The limits of detection were 0.04 μM and 1.3 μM for BP-3 and 3MOP, respectively (Table S2). The calibration curves were generated by calculating the peak area versus the concentration of each target compound (Table S3).

Mass spectrum analyses were performed on a 1290 Infinity II HPLC equipped with a C_{18} reversed-phase column (4.6 × 250 mm, 5 μm; Agilent technologies., CA, USA), coupled with a Quadrupole Time of Flight (Q-TOF) high resolution mass spectrometer (Agilent technologies., CA, USA). The mobile phase consisted of water containing 0.1 % formic acid (A) and acetonitrile (B). The flow rate was set at 0.4 mL/min. The running program was 0–15 min, 10–95 % of B, then holding for 10 min. Under these conditions, peaks corresponding to BP-3 and 3MOP appeared at 21.9 min and 14.4 min, respectively. The column temperature was maintained at 25 ± 2 °C.

Gas chromatography-mass spectrometry (GC-MS) analysis was performed on an Agilent 7890B gas chromatography equipped with an HP-5MS capillary column (30 m × 0.25 mm × 0.25 μm film thickness, Agilent technologies., CA, USA). The column temperature gradient was as follows: 0–2 min, 50 ℃; 2–28 min, 130 ℃; 28–33 min, 180 ℃; and 33–54 min, 285 ℃, holding for 5 min. The injection port maintained at 280 °C. Samples were extracted using three volumes of ethyl acetate. The fractions containing the products were collected and evaporated to dryness. The dried samples were dissolved in ethyl acetate and mixed with equal volume of *N,O*-bis (trimethylsilyl) trifluoroacetamide (BSTFA) for trimethylsilyl (TMS) derivatization at 60 °C for 30 min before GC-MS analysis.

2.9. Data availability

The metagenomic data have been deposited in the NCBI database under BioProject accession number PRJNA1170462. The assembled MAG1 and MAG2 sequences are available under the accession numbers ASM4879957v1 and ASM4879956v1, respectively.

3. Results and discussion

3.1. BP-3 degradation by the aerobic enrichment culture from WWTP

A small-scale microcosm with BP-3 under aerobic conditions was operated by inoculating with the activated sludge from the aerobic tank of a WWTP. After four months of continuous transfer, an enrichment culture exhibiting efficient degradation capacity for BP-3 was obtained. This degradation was accompanied by visible biomass accumulation when BP-3 was supplied as the sole carbon and energy source. As shown in Fig. 2A, BP-3 degradation by the enriched consortium did not exhibit an evident lag phase and proceeded to complete removal within 24 h, with an apparent degradation rate of 6.3 ± 0.5 μmol L^{-1} h^{-1}. When inoculated with autoclaved enrichment cultures, no change in BP-3 concentration in these controls was observed indicating negligible sorption and volatilization losses.

3.2. Identification of the catabolic intermediate at community level

During degradation of BP-3 by the aforementioned enriched consortium, a UV–visible transient intermediate product (λ_{max} at 220 nm and 276 nm) with a retention time of 14.4 min was observed by high performance liquid chromatography (HPLC) analysis under conditions specified in the Methods section, however, this peak was not observed in the control experiment inoculated with autoclaved enrichment culture (Fig. 2A; Figure S1). This intermediate product could not be assigned to any of the previously reported BP-3 degrading products such as BP-1 [26] or ring-hydroxylating products [25], implying that BP-3 is likely to be degraded by the consortium through an uncharacterized catabolic pathway. High resolution mass spectrum analysis produced a molecular formula $C_7H_8O_2$ which is inferred to be 3-methoxyphenol (3MOP) based on the comparison of retention time (14.4 min) and mass spectra ($[M + H]^+$=125.0597, mass accuracy: 0.799 parts per million [ppm] error) with those of authentic 3MOP (Figure S1). Moreover, this product was also detected by GC-MS analysis of the acidic extract of the enrichment cultures. Based on the extracted ion chromatogram and fragmentation pattern of mass spectrum, the product was also identified as 3MOP (Figure S2). The intermediate product 3MOP reached maximum accumulation concentration at ~18 h, and gradually disappeared within 50 h (Fig. 2A), indicating that 3MOP is finally degraded by the bacterial consortium. The degradation of 3MOP is also subsequently demonstrated by the successful isolation of a 3MOP utilizer from the consortium (see below).

3.3. Metagenome-guided isolation and characterization of BP-3 degrading strains

In order to reveal the microbial composition of the BP-3-degrading consortium, species analysis was performed on the sequentially transferred enrichment cultures. The results showed that the composition of the BP-3-degrading consortium remained stable across transfers, predominantly consisting of the genera *Pigmentiphaga* and *Brucella* (Fig. 2B). These two genera accounted for an average abundance as high as 98.2 %. Other classic xenobiotics-degrading microorganisms, such as those from the genera *Pseudomonas*, *Burkholderia*, and *Bacillus*, were also present but in very small proportions (Fig. 2B).

To investigate the specific bacterial strains contributing to BP-3 degradation, pure cultures from the consortium were isolated using the dilution separation method. A total of six colonies in two

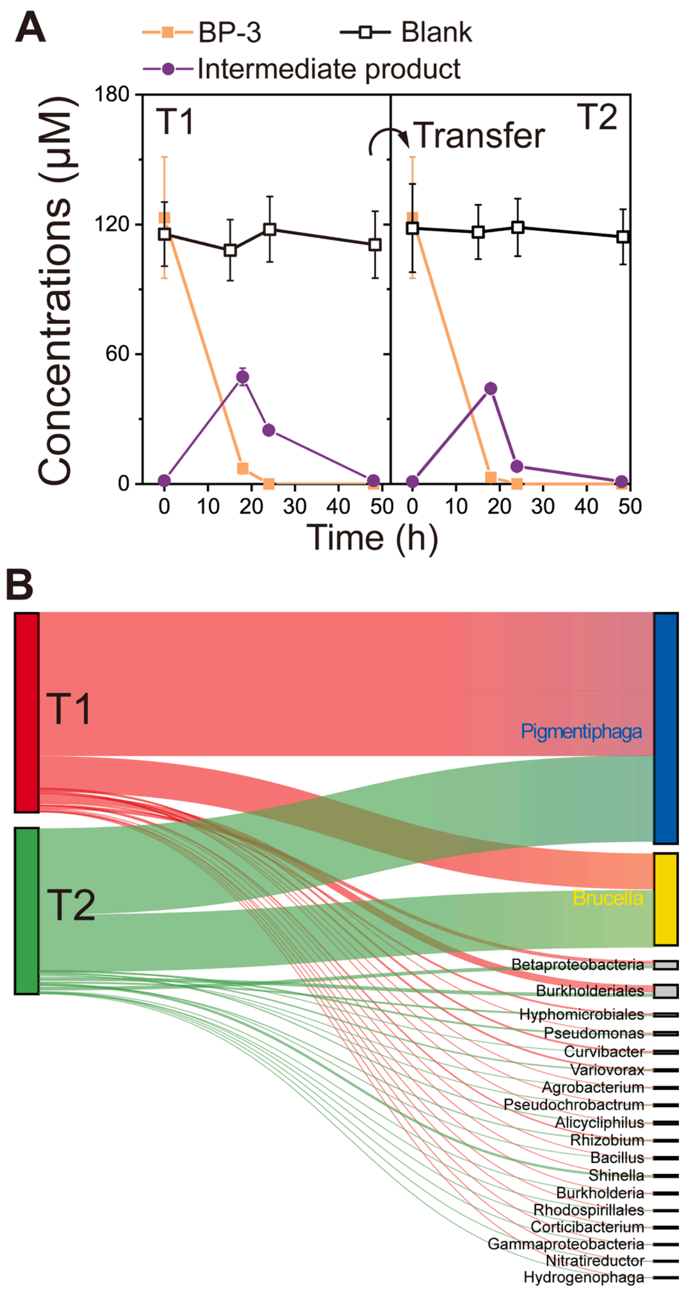

Fig. 2. BP-3 degradation by a bacterial consortium from WWTP. (A) Degradation of BP-3 by two sequential transfers (T1 and T2) of a consortium enriched from WWTP. A UV–visible intermediate product (purple line) is observed during the degradation process. The intermediate product was later identified to be 3-methoxyphenol. (B) Bacterial composition of the BP-3 degrading consortium analyzed by metagenomic sequencing. Both T1 and T2 were dominated by *Pigmentiphaga* and *Brucella*.

morphologies were spiked for culturing and subsequently analyzed by 16S rRNA gene sequencing. All of the colonies were identified as species belonging to genera either *Pigmentiphaga* or *Brucella*, which represent the two dominating bacteria of the consortium as suggested by the community structure analysis (Fig. 2B). These strains haven't previously been reported to have BP-3-degrading abilities. Based on the growth experiments using BP-3 or its metabolite 3MOP as substrates, it was observed that the isolates belonging to the genus *Pigmentiphaga* could utilize BP-3, but not 3MOP, as sole carbon and energy source for growth. In contrast, the isolates belonging to the genus *Brucella* could only grow with 3MOP. Thereafter, we selected two representative isolates, designated *Pigmentiphaga* sp. strain NyZ216 and *Brucella* sp. strain NyZ218, for further analyses. As shown in Fig. 3, *Pigmentiphaga* sp. strain NyZ216 is a rod-shaped, Gram-negative bacterium that is most closely related to the *Pigmentiphaga daeguensis* K110 [32]. *Brucella* sp. strain NyZ218 is also a rod-shaped bacterium but with active exopolysaccharide-producing ability. The strains NyZ216 and NyZ218 exhibited a significantly different growth pattern in rich medium (TSB), with doubling times of 4 h and 1.5 h, respectively, and maximum $OD_{600\ nm}$ values of 0.02 and 0.3, respectively.

3.4. Growth and degradation experiments by the pure isolates

Although strain NyZ216 alone could use BP-3 as sole carbon source for growth, the total biomass is obviously less than that of the consortium (Fig. 4A). Moreover, the BP-3 degradation rate by strain NyZ216 is also lower than that of the enrichment culture (Fig. 2A; Fig. 4A), with a ~15 h lag phase observed for the BP-3 degradation (Fig. 4A). Strain NyZ216 could not degrade other organic UV filters structurally analogous to BP-3, including BP, BP-1, BP-2, BP-4, BP-5, BP-6, BP-7 and BP-8 (Figure S3). Degradation of BP-3 by NyZ216 accompanied with stoichiometrically formation of 3MOP as a dead-end product (Figure 4A1), which is also implied by its incapability of growing on 3MOP (Figure 4B1). In contrast, strain NyZ218 featured with its ability to grow on 3MOP but not BP-3 (Figure 4A2 and Figure 4B2).

During the growth of NyZ216 on BP-3, no other UV–visible product than 3MOP was observed in the culture by HPLC analysis. In order to identify the fate of the other moiety from BP-3 degradation, we performed an enzyme assay using the cell extracts of BP-3-growing NyZ216 cells. The enzyme assay revealed a 3MOP product identical to the one detected in the growth experiments. Unexpectedly, a new product with a retention time of 10.2 min appeared in the chromatogram of HPLC analysis (Figure S4A). We tentatively assigned the product to be benzoic acid (BA) due to its identical retention time and UV spectra to authentic BA. Time course analysis confirmed that equal molar amount of 3MOP and BA were formed during the degradation of BP-3 (Figure S4B). Growth assays indicated that NyZ216 readily uses BA as sole carbon and energy source for growth, whereas NyZ218 is unable to utilize BA (Figure S4C). Overall, the above results showed that the degradation of BP-3 by NyZ216 produces BA and 3MOP, with the former supporting the growth of the strain and the latter being a dead-end product, but utilized by strain NyZ218.

3.5. Reconstruction of BP-3-degrading consortium

We further constructed a two-strain synthetic consortium (SynC) consisting of strains NyZ216 and NyZ218 for evaluating its BP-3 degradation performance. The two-strain consortium is adequate for BP-3 degradation without 3MOP accumulation, and the reconstructed consortium exhibits similar degradation performance to the natural consortium (Fig. 2A and Fig. 4 A3). Using BP-3 or 3MOP as growth substrates, the constructed consortium showed a significantly higher biomass accumulation compared the single strain alone (Fig. 4). The two-strain consortium had a higher BP-3 degradation efficiency than that of the strain NyZ216 alone during growth experiments (Fig. 4A), this might be partially due to that the degradation of dead-end product 3MOP by strain NyZ218 alleviated the product inhibition. Nonetheless, other factors such as cell contact, metabolite cross-feeding might also be important for the degradation process. Unexpectedly, we noted that the presence of strain NyZ216 promotes the growth and utilization of NyZ218 on 3MOP (Fig. 4B), the underlying mechanism supporting the enhancement is yet unknown. All together, these results revealed the synergistic interactions of strains NyZ216 and NyZ218 for the degradation of BP-3.

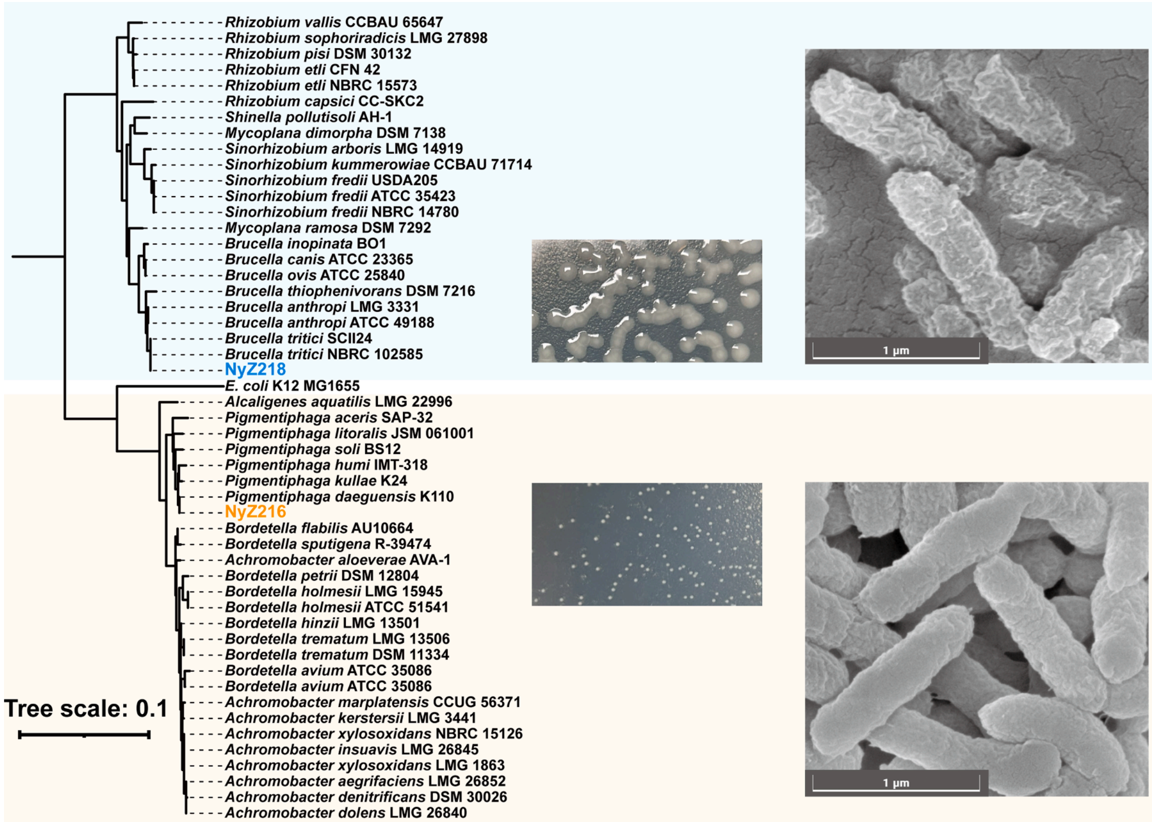

Fig. 3. Isolation of pure cultures from the BP-3-degrading consortium. 16S rRNA gene sequences-based phylogenetic tree (left) of *Pigmentiphaga* sp. strain NyZ216 and *Brucella* sp. strain NyZ218 and their relatives. The colonial morphology after 48 h of growth on TSB plates (middle) and cellular morphologies under scanning electron microscopy (right) are shown.

3.6. Metagenome-based reconstruction of the catabolic pathway

To profile the microbial metabolic capability, the metagenomic raw reads obtained from two sequentially transferred consortia metagenomic libraries were assembled into metagenomes. Two assembled genomes (MAG1 and MAG2), with completeness >99 % and contamination <1 %, were retrieved from each library (Table 1 and Table S4). The two MAGs belong to the genera *Pigmentiphaga* and *Brucella*, which are exactly consistent to the isolated bacterial strains NyZ216 (MAG1) and NyZ218 (MAG2), respectively. Based on gene function annotation of the assembled genomes, a large number of aromatic catabolism genes are present in the two genomes. Notably, genes related to benzoate degradation are identified in MAG1, including the complete set genes of dioxygenation pathway and benzoyl-CoA pathway (Table S5). However, the benzoate-degrading genes are absent from genome of MAG2, consistent with the growth inability of NyZ218 on benzoate. On the other hand, the presence of a resorcinol-degrading gene cluster in MAG2, encoding enzymes including resorcinol hydroxylase (GraAD), hydroxyquinol 1,2-dioxygenase (GraB) and maleylacetate reductase (GraC) indicated that the resorcinol is likely an intermediate resulted from the initial reaction of 3MOP catabolism in strain NyZ218 (Table S6). It would be reasonable to speculate that resorcinol is formed through demethylation of 3MOP by an unknown demethylase in its initial degradation step (Fig. 5). Additionally, the enzyme responsible for the initial step of BP-3 breakdown has not been reported previously, either oxygenase or hydrolase is plausible candidate for this process. Heterologous expression of all four annotated C–C hydrolases from the MAG1 genome did not confer BP-3 degradation activity in *E. coli* cells. To directly isolate the enzyme, we employed a multi-step protein purification protocol. Despite significant effort, the active fractions consistently contained a mixture of proteins, and no single band could be definitively linked to the hydrolase activity. This suggests the enzyme is expressed at low level or may be a fragile multi-component system, making its purification exceptionally challenging. Nevertheless, further molecular and biochemical analyses will be required for revealing the functional gene and enzyme for the C-C cleavage of BP-3 in strain NyZ216 and demethylation of 3MOP in strain NyZ218.

3.7. BP-3 degradation conditions and performance in the real wastewater

During the BP-3 degradation experiments, the optimal conditions for the single strain NyZ216 or the mixture of strains NyZ216 and NyZ218 were similar, with a preferred pH of ~9.0 and a temperature of ~37 ℃ (Figure S5). The degradation performance is likely to be increased by accelerating enzymatic activity due to climate change in summer which often exceed 30 °C. Figure S6 shows the best fit of the BP-3 degradation rates under environmental relevant concentrations to the Michaelis-Menten equation. For the single strain NyZ216 and the mixture of strains NyZ216 and NyZ218, the V_{max} was 33.55 and 28.92 μM^{-1} h^{-1}, respectively; and the K_m values were 0.083 and 0.080 mM, respectively.

To assess the capabilities of indigenous wastewater microorganisms for BP-3 degradation through the 3MOP pathway characterized here, we tested a total of 14 WWTPs wastewater samples (designated WW1 to WW14) sourced from geographically diverse regions in China. The detailed information of sampling sites were listed in Table S1. After 18 days of incubation, most of the cultures (9 out of 14) exhibited evident BP-3 degradation activity with varying degrees (43.8 %-99.8 %), and degradation of BP-3 in the remaining five cultures is negligible (Fig. 6A). These results indicate that the degradation capacity of BP-3 varies greatly in WWTPs from different regions. Notably, of the 9 cultures with BP-3-degrading capacity, 3MOP was only detected as an intermediate product in the WWTP wastewater sample from Wuhan city (designated

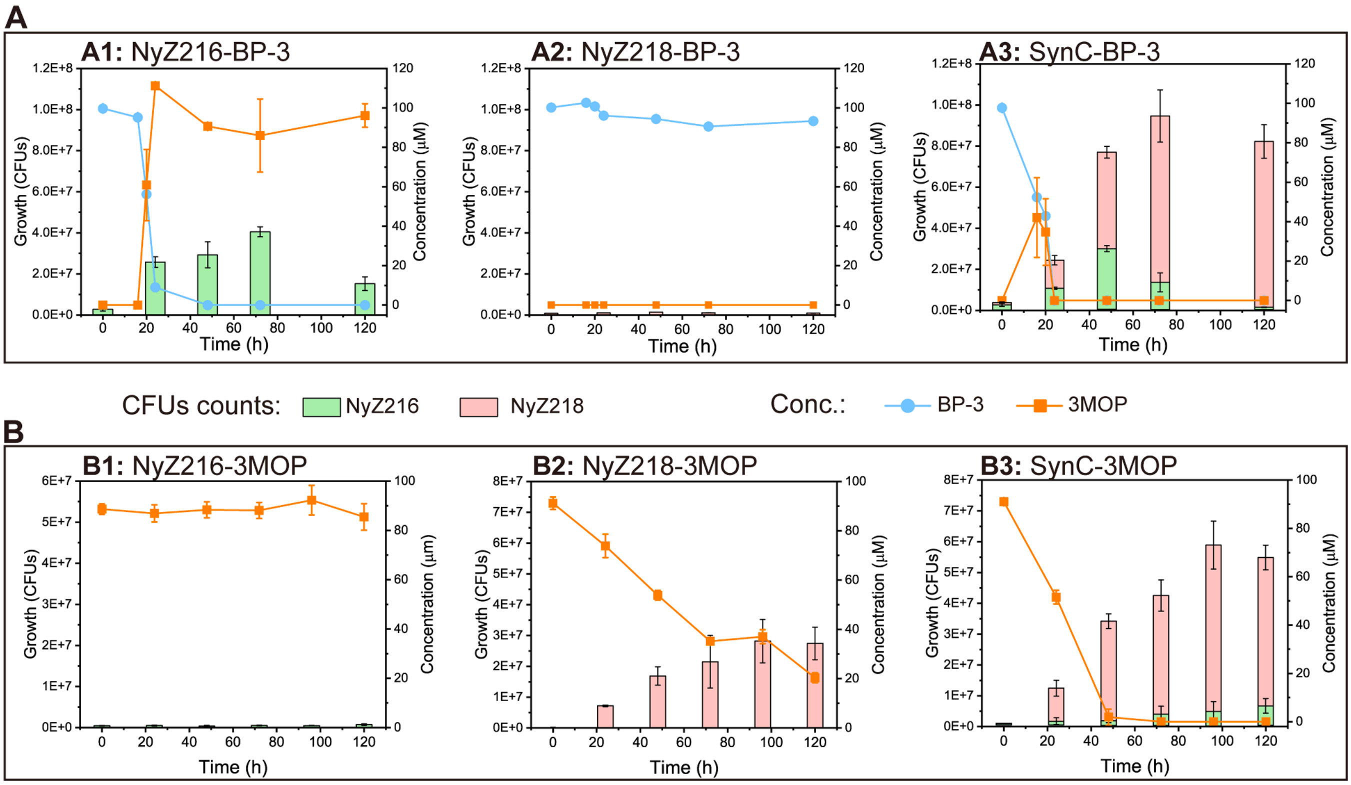

Fig. 4. Growth and degradation characteristics of pure cultures and synthetic consortium on BP-3 and 3MOP. "SynC" means the synthetic consortium by strains NyZ216 and NyZ218. The concentration is shown as line, and growth is shown as histogram by cell densities (CFUs mL^{-1}). (A) BP-3 degradation and formation of intermediate 3MOP during growth on BP-3 with strain NyZ216 (A1), strain NyZ218 (A2) or consortium SynC (A3). (B) Degradation of 3MOP during growth on 3MOP with strain NyZ216 (B1), strain NyZ218 (B2) or consortium SynC (B3).

Table 1
Information of the assembled MAGs from metagenomic sequencing of BP-3-degrading consortium.

MAG name	Annotation (genus)	Genome size (Mbp)	Completeness (%)	Contamination (%)	GC content
MAG1	*Pigmentiphaga*	5.6	99.09	0.907	67.7 %
MAG2	*Brucella*	5.5	99.59	0.875	56.2 %

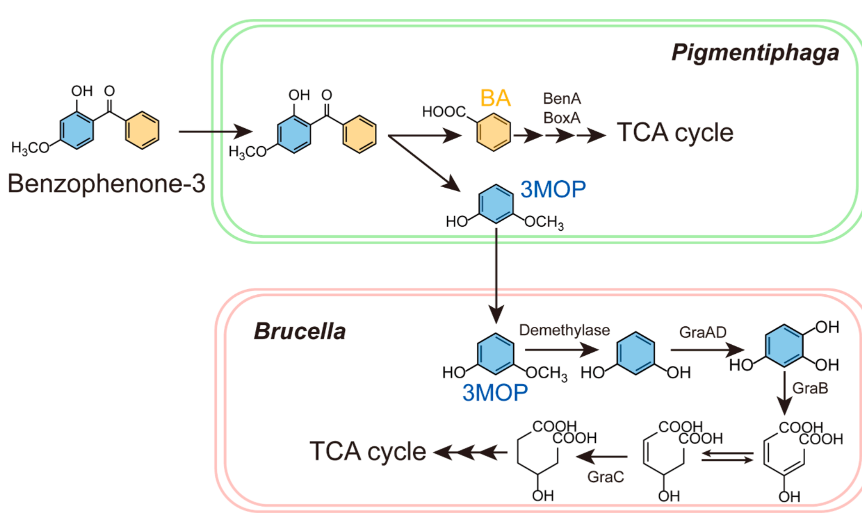

Fig. 5. Proposed catabolic interaction model for the synergistic degradation of BP-3 and its metabolites by *Pigmentiphaga* and *Brucella* strains from WWTPs.

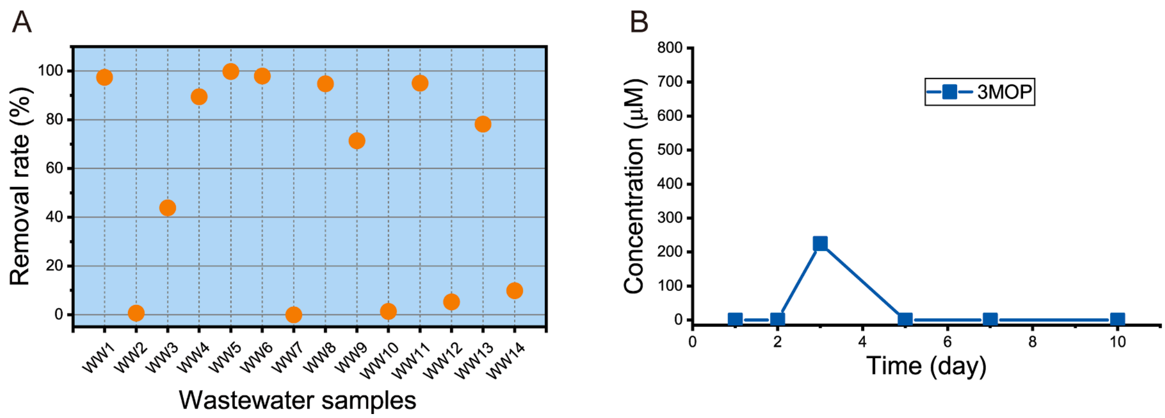

Fig. 6. Microbial degradation capacities of BP-3 in wastewater-derived microbial cultures from different WWTPs in China. (A) BP-3 removal rate by indigenous microbes from 14 wastewater samples. Results are presented as the average of three replicates, with standard deviations of less than ±10 %. (B) The formation of the catabolic intermediate 3MOP in sample WW11. 3MOP was below the detection limit in the other 13 cultures.

WW11) (Fig. 6B), indicating other BP-3 degradation pathway might be present in the cultures except WW11, and the 3MOP-pathway characterized here seem not a prevalent BP-3 degradation pathway in WWTPs.

The degradation of BP-3 by the strains NyZ216 and NyZ218 in the real wastewater without BP-3-degrading indigenous microorganism was further investigated. The wastewater or sterile wastewater without inoculation of isolated BP-3-degrading strains showed no change in BP-3 concentration, indicating that removal of BP-3 in the wastewater by natural processes such as volatilization, biodegradation, and adsorption was negligible. After adding consortium consisting of NyZ216 and NyZ218 into the wastewater, the degradation of BP-3 was evident with a rate of 9.7 μM^{-1} h^{-1}, indicating a potential for application of the strains in wastewater treatment (Figure S7).

4. Conclusion

Here, we used high-throughput metagenomic sequencing to characterize the BP-3-enriched degrading consortium and recovered MAGs to identify BP-3-degrading bacteria. Two isolates (*Pigmentiphaga* sp. strain NyZ216 and *Brucella* sp. strain NyZ218) consisting of the dominating species of the consortium were isolated and identified. Degradation experiments using the isolated strains showed that strain NyZ216 readily degraded BP-3 with the accumulation of a dead-end product 3MOP, while strain NyZ218 could utilize 3MOP as sole carbon and energy source for growth. Under co-occurrence of strains NyZ216 and NyZ218, BP-3 and its intermediates were degraded as confirmed by the consortium reconstruction assays. In regard to the newly characterized degraders here, BP-3 breakdown is initialized by cleaving the carbonyl group resulting in the formation of 3MOP and benzoate, both of which are naturally-occurring compounds, and could be easily assimilated by various environmental microorganisms. Because of the benzophenone-type UV filters sharing a common carbonyl group-containing structure with BP-3, the pathway characterized here is promising for application to the removal of other benzophenone-type UV filters through appropriately engineering of the BP-3 degradation pathway. This could be accelerated by the further studies for experimental validation of the functional genes and enzymes in BP-3 degraders.

CRediT authorship contribution statement

Tao Li: Writing – review & editing, Visualization, Project administration, Funding acquisition, Data curation, Conceptualization. **Piaopiao Pan:** Software. **Ning-Yi Zhou:** Writing – review & editing, Supervision, Conceptualization. **Ao Zhang:** Writing – original draft, Visualization, Software, Methodology, Investigation, Funding acquisition, Formal analysis.

Environmental implication

The widespread use of benzophenone-3 (BP-3) in various consumer products has led to contamination of environments. BP-3 is being detected in wastewater effluent, lakes, rivers and coastal waters, and is recognized as an emerging organic pollutant with toxic effects, particularly as an endocrine disruptor. Here, we identified a novel BP-3 bacterial biodegradation pathway, which yields two naturally occurring compounds 3-methoxyphenol (3MOP) and benzoate via C-C bond cleavage. These findings provide new insights into the microbial interactions driving the environmental transformation of this globally concerning pollutant, and also offering a potential strategy for BP-3-contaminated wastewater treatment by harnessing bacterial consortia.

Declaration of Competing Interest

The authors declare that they have no known competing financial interests or personal relationships that could have appeared to influence the work reported in this paper.

Acknowledgments

This work was supported by the National Key R&D Program of China (grant number 2021YFA0910300); the National Natural Science Foundation of China (NSFC) (grant number 32400080). We would like to thank Dr. Jingli Dai for highlighting the urgency of eliminating the organic UV filters from the environment.

Appendix A. Supporting information

Supplementary data associated with this article can be found in the online version at doi:10.1016/j.jhazmat.2025.140176.

Data availability

Data will be made available on request.

References

[1] Janssen, D.B., Dinkla, I.J., Poelarends, G.J., Terpstra, P., 2005. Bacterial degradation of xenobiotic compounds: evolution and distribution of novel enzyme activities. Environ Microbiol 7, 1868–1882.
[2] Adamu Suleiman, K., Bichi, Y.H., Nasiru, A.Y., Babangida, A., Umar, M.M., Muhammad, R., 2023. Review: synthetic microbial consortia in bioremediation and biodegradation. Int J Res Innov Appl Sci VIII, 232–241.
[3] American Chemical Society, Oxybenzone information. ⟨https://www.acs.org/content/acs/en/molecule-of-the-week/archive/o/oxybenzone.html⟩ 2018, Accessed 26 May 2024.

[4] United States Environmental Protection Agency. The United States High Production Volume (USHPV) database. ⟨https://comptox.epa.gov/dashboard/chemical/details/DTXSID3022405?list=EPAHPV⟩ 2024. Accessed 26 May 2024.
[5] Mao, J.F., He, Y., Gin, K., 2019. Occurrence and fate of benzophenone-type UV filters in aquatic environments: a review. Environ Sci Water Res Technol 5, *209–223*.
[6] Duis, K., Junker, T., Coors, A., 2021. Review of the environmental fate and effects of two UV filter substances used in cosmetic products. Sci Total Environ 808, 151931.
[7] Carstensen, L., Zippel, R., Fiskal, R., Börnick, H., Schmalz, V., Schubert, S., et al., 2023. Trace analysis of benzophenone-type UV filters in water and their effects on human estrogen and androgen receptors. J Hazard Mater 456, 131617.
[8] Mozas-Blanco, S., Rodriguez-Gil, J.L., Kalman, J., Quintana, G., Díaz-Cruz, M., Rico, A., et al., 2023. Occurrence and ecological risk assessment of organic UV filters in coastal waters of the iberian peninsula. Mar Pollut Bull 196, 115644.
[9] Barros, D., Nascimento, G., Okon, C., Rocha, M., Santo, D., Feitoza, L., et al., 2023. Benzophenone-3 sunscreen causes phytotoxicity and cytogenotoxicity in higher plants. Environ Sci Pollut Res 30, 112788–112798.
[10] Yao, Y.-N., Wang, Y., Zhang, H., Gao, Y., Zhang, T., Kannan, K., 2024. A review of sources, pathways, and toxic effects of human exposure to benzophenone ultraviolet light filters. Eco Environ Health 3, 30–44.
[11] Mustieles, V., Balogh, R.K., Axelstad, M., Montazeri, P., Márquez, S., Vrijheid, M., et al., 2023. Benzophenone-3: comprehensive review of the toxicological and human evidence with meta-analysis of human biomonitoring studies. Environ Int 173, 107739.
[12] Schildroth, S., Bethea, T.N., Wesselink, A.K., Friedman, A., Fruh, V., Calafat, A.M., et al., 2024. Personal care products, socioeconomic status, and endocrine-disrupting chemical mixtures in llack women. Environ Sci Technol 58, 3641–3653.
[13] Silva, E., Mínguez-Alarcón, L., Coull, B., Hart, J., James-Todd, T., Calafat, A., et al., 2024. Benzophenone-3 and ovarian reserve. Fertil Steril 122, 494–503.
[14] Ma, J., Wang, Z., Qin, C., Wang, T., Hu, X., Ling, W., 2023. Safety of benzophenone-type UV filters: a mini review focusing on carcinogenicity, reproductive and developmental toxicity. Chemosphere 326, 138455.
[15] S. d. S, Almeida, Rocha, T.L., Qualhato, G., L. d. A. R, Oliveira, C. L. d, Amaral, E. C. d, Conceição, et al., 2019. Acute exposure to environmentally relevant concentrations of benzophenone-3 induced genotoxicity in poecilia reticulata. Aquat Toxicol 216, 105293.
[16] Wijgerde, T., Ballegooijen, M., Nijland, R., van der Loos, L., Kwadijk, C., Osinga, R., et al., 2020. Adding insult to injury: effects of chronic oxybenzone exposure and elevated temperature on two reef-building corals. Sci Total Environ 733, 139030.
[17] Mitchelmore, C., Burns, E., Conway, A., Heyes, A., Davies, I., 2021. A critical review of organic ultraviolet filter exposure, hazard, and risk to corals. Environ Toxicol Chem 40, 967–988.
[18] Sun, J., Rene, E., Danyang, T., Lu, Y., Jin, Q., Lam, J.C.-H., et al., 2023. Degradation of organic UV filters in the water environment: a concise review on the mechanism, toxicity, and technologies. J Hazard Mater 463, 132822.
[19] Manasfi, T., Storck, V., Ravier, S., Demelas, C., Coulomb, B., Boudenne, J.L., 2015. Degradation products of benzophenone-3 in chlorinated seawater swimming pools. Environ Sci Technol 49, 9308–9316.
[20] Manasfi, T., Coulomb, B., Ravier, S., Boudenne, J.L., 2017. Degradation of organic UV filters in chlorinated seawater swimming pools: transformation pathways and bromoform formation. Environ Sci Technol 51, 13580–13591.
[21] Lu, Y., Chow, M.K., Sun, J., Tao, D., Jin, Q., Ren, Y., et al., 2023. Identification of transformation products of organic UV filters by photooxidation and their differential estrogenicity assessment. Environ Sci Technol 57, 17110–17122.
[22] Wang, Y., Jiang, S., Chen, X., Liu, X., Li, N., Nie, Y., et al., 2023. Comparison of developmental toxicity of benzophenone-3 and its metabolite benzophenone-8 in zebrafish. Aquat Toxicol 258, 106515.
[23] Jou-Claus, S., Rodríguez-Escales, P., Martínez-Landa, L., Diaz-Cruz, M.S., Carrera, J., Sunyer-Caldú, A., et al., 2024. Assessing the fate of benzophenone-type UV filters and transformation products during soil aquifer treatment: the biofilm compartment as bioaccumulator and biodegrader in porous media. Environ Sci Technol 58, 5472–5482.
[24] Ramos, S., Homem, V., Alves, A., Santos, L., 2015. A review of organic UV-filters in wastewater treatment plants. Environ Int 86, 24–44.
[25] Fagervold, S.K., Rohée, C., Rodrigues, A.M.S., Stien, D., Lebaron, P., 2021. Efficient degradation of the organic UV filter benzophenone-3 by *Sphingomonas wittichii* strain BP14P isolated from WWTP sludge. Sci Total Environ 758, 143674.
[26] Baek, J.H., Kim, K.H., Lee, Y., Jeong, S.E., Jin, H.M., Jia, B., et al., 2022. Elucidating the biodegradation pathway and catabolic genes of benzophenone-3 in *Rhodococcus* sp. S2-17. Environ Pollut 299, 118890.
[27] Jin, C., Geng, Z., Pang, X., Zhang, Y., Wang, G., Ji, J., et al., 2019. Isolation and characterization of a novel benzophenone-3-degrading bacterium *Methylophilus* sp. Strain FP-6. Ecotox Environ Safe 186, 109780.
[28] Huang, Y., Law, C.F.J., Lam, T.-K., Leung, K., 2021. Risks of organic UV filters: a review of environmental and human health concern studies. Sci Total Environ 755, 142486.
[29] Li, T., Xu, Z.-J., Zhou, N.-Y., 2023. Aerobic degradation of the antidiabetic drug metformin by *Aminobacter* sp. Strain NyZ550 Environ Sci Technol 57, 1510–1519.
[30] Li, T., Xu, Z.-J., Zhang, S.-T., Xu, J., Pan, P., Zhou, N.-Y., 2024. Discovery of a Ni^{2+}-dependent heterohexameric metformin hydrolase. Nat Commun 15, 6121.
[31] Tamura, K., Stecher, G., Kumar, S., 2021. MEGA11: molecular evolutionary genetics analysis version 11. Mol Biol Evol 38, 3022–3027.
[32] Yoon, J.H., Kang, S.J., Kim, W., Oh, T.K., 2007. *Pigmentiphaga daeguensis* sp. Nov., isolated from wastewater of a dye works, and emended description of the genus *Pigmentiphaga*. Int J Syst Evol Microbiol 57, 1188–1191.